
DERM12345: A LARGE, MULTISOURCE DERMATOSCOPIC SKIN LESION DATASET WITH 38 SUBCLASSES

Abdurrahim Yilmaz¹

Sirin Pekcan Yasar²

Gulsum Gencoglan^{3,†}

Burak Temelkuran^{1,†}

1. Department of Metabolism, Digestion, and Reproduction, Imperial College London, London, SW7 2AZ, United Kingdom

2. Department of Dermatology, The University of Health Sciences, Haydarpaşa Numune Research and Training Hospital, Istanbul, 34668, Türkiye

3. Department of Dermatology, Işinye University, Liv Hospital Vadistanbul, Istanbul, 34010, Türkiye

Corresponding authors: Gulsum Gencoglan (ggencoglan@gmail.com), Burak Temelkuran (b.temelkuran@imperial.ac.uk)

ABSTRACT

Skin lesion datasets provide essential information for understanding various skin conditions and developing effective diagnostic tools. They aid the artificial intelligence-based early detection of skin cancer, facilitate treatment planning, and contribute to medical education and research. Published large datasets have partially coverage the subclassifications of the skin lesions. This limitation highlights the need for more expansive and varied datasets to reduce false predictions and help improve the failure analysis for skin lesions. This study presents a diverse dataset comprising 12,345 dermatoscopic images with 38 subclasses of skin lesions collected in Türkiye which comprises different skin types in the transition zone between Europe and Asia. Each subgroup contains high-resolution photos and expert annotations, providing a strong and reliable basis for future research. The detailed analysis of each subgroup provided in this study facilitates targeted research endeavors and enhances the depth of understanding regarding the skin lesions. This dataset distinguishes itself through a diverse structure with 5 super classes, 15 main classes, 38 subclasses and its 12,345 high-resolution dermatoscopic images.

Keywords Dermatology · Skin Lesion Dataset · Skin Cancer · Subclasses of Skin Lesions · Artificial Intelligence · Deep Learning

Background & Summary

Dermatology, also known as epiluminescence microscopy, is the inspection of the skin using magnifying lenses and polarized or non-polarized filtered illumination, allowing examination of lesions invisible to the naked eye. It is the most extensively used and standardized diagnostic procedure in clinics to diagnose skin lesions. Various types of dermatoscopes are actively used in daily clinics. Hand-held dermatoscopes, for example, have become widely available, affordable, and widely employed, especially in developing countries. However, dermatologists' diagnostic performance in dermatoscopic skin lesion identification is closely linked to their training and prior clinical experience, highlighting a variability inherent in human decisions. The prevalence and structure of malignant and benign lesions that vary depending on race, geographical factors and skin type also affects dermatologists' performance. Addressing this gap, artificial intelligence (AI) trained on specialized dataset can reduce the experience gap that results from the human factor during the clinical examination of these lesions [1].

One of the initial studies was published on the classification of only three classes: melanoma, nevus, and seborrheic keratosis [2, 3]. The skin lesion dataset HAM10000, which had seven classes and common lesions, was published in 2018 [4]. Eight classes with the squamous cell carcinoma skin lesion which is a common lesion but uncovered in HAM10000 was later presented by the BCN20000 dataset [5]. Among dermatoscopic skin lesion datasets, BCN20000

has the largest number of multi-class images (eight classes), still requires further development and expansion to include subclasses. New datasets are continued to be published in open access repositories such as The International Skin Imaging Collaboration (ISIC), which currently has a total of 76,108 public images (accessed at: 30 May 2024) [6, 7]. Publishing new datasets enables the development of more robust and intelligent AI algorithms with different approaches.

Datasets on skin lesions can be listed in four different categories: clinical, pathological slide, and dermatoscopic image datasets, and datasets combining more than one of these modalities. Clinical image datasets such as the Interactive Atlas of Dermatoscopy and the Dermofit Image Library can be accessible for a fee [8, 9]. The MED-NODE Dataset [10], the Asan and Hallym Dataset [11], the SD-198/SD-260 Datasets [12, 13, 14], PAD-UFES-20 [15], SCIN (5.2% skin lesion) [16], Atlas Dermatologica [17], and DermaAmin [18] are all open-access. Fitzpatrick 17k Dataset is a dataset sourced from Atlas Dermatologica and DermaAmin, with the addition of Fitzpatrick skin type information (28.62% skin lesion) [19]. Diverse dermatology images (DDI) dataset also presents skin images with their skin type [20]. Cancer Genome Atlas is a pathological slide image dataset for skin lesions in the literature [21]. Clinical, dermatoscopic, and pathological images can all be found on Dermnet NZ for a free (high-resolution images for a fee) [22]. Study results show that the diagnostic accuracy (by clinicians and AI) achievable using dermatoscopic image datasets result in higher success rates when compared to those achievable using clinical image datasets, bringing out the importance of the dermatoscopic image datasets [23]. Pathological images require tissue excision from the patient. For that reason, pathological image dataset is not as practical as dermatoscopic observation.

PH² dataset was published for benchmarking dermatoscopic images including with three lesion classes (common nevus, atypical nevus and melanoma (mel)) [24]. The Derm7pt dataset with five lesion classes (basal cell carcinoma (bcc), mel, miscellaneous, nevus (nv), and seborrheic keratosis (sk)), 2000 dermatoscopic and clinical images was published along with the 7-point checklist pattern analysis and its automation by using artificial neural networks [25]. The largest dermatoscopic dataset included in the scientific studies is the International Skin Imaging Collaboration (ISIC) archive with 240,000+ total images (accessed at: 30 May 2024). This archive contains these datasets: ISIC-2016 with 1,279 images and two lesion classes (benign and malignant) [2], ISIC-2017 with 2,000 images three lesion classes (mel, nv, and sk) [3], ISIC-2018 [26] and HAM10000 with 10,015 images and seven lesion classes (akiec, bcc, benign-keratosis like (bkl), dermatofibroma (df), mel, nv, and vascular (vasc)) [4], BCN20000 with 19,424 images and eight lesion classes (actinic keratosis (ak), bcc, df, mel, nv, squamous cell carcinoma (scc), sk, and vasc) [5] and Patient-Centric dataset with 33,126 images and two lesion classes (benign and mel) [27]. Lastly, the dataset collected in Argentina with 10 subclasses (ak, bcc, df, mel, nv, scc, sk, solar lentigo (sl), lichenoid keratosis (lk), and vasc) was added into ISIC dataset [6]. Between 2016 and 2020, numerous competitions were held on challenges such as lesion segmentation, feature extraction, and lesion classification, using these ISIC datasets.

These large datasets are crucial for the development of AI based models for skin lesion classification purposes. In addition, the introduction of subclass annotations in skin image datasets has high potential to enhance studies in the AI field focusing on skin disease, for creation of more trustworthy, robust, and intelligent systems. Here, our study presents a taxonomic tree for skin lesion classes and a dataset of 38 skin lesions annotated with subclasses for the first time in the scientific literature. This dataset, which contains a total of 12,345 images, is a comprehensive dermatoscopic image dataset available. Moreover, this is the one of the largest collection to date in terms of the total number of images in multiclass datasets.

Methods

The DERM38 dataset contains 12,345 high-resolution dermatoscopic images from 1,761 patients, which were collected from 2008 to 2020 in the Department of Dermatology and Venerology at Celal Bayar University (Manisa, Türkiye), Istinye University (Istanbul, Türkiye) and University of Health Sciences Haydarpasa Numune Research and Training Hospital (Istanbul, Türkiye) by using MoleMax 3, MoleMax HD (Derma Medical Systems, Vienna, Austria), FotoFinder® videodermatoscope (FotoFinder Systems, Bad Birnbach, Germany) and 3gen Dermlite DL4 hand-held dermatoscopes (DermLite LLC, California, United States of America) with connection kit for iPhone 5 and 7 (Apple Inc., California, United States of America). Ethical approval of images was based on ethics review board protocols 20.478.486/1023 (Manisa Celal Bayar University, 24/11/2021). The informed consent was waived because of the retrospective nature of the study as the dataset contains anonymized data. The final dataset includes 38 skin lesion classes. The collection process includes capturing a wide variety of skin lesions using both digital dermatoscopy devices and high-resolution digital single-lens reflex (DSLR) cameras with dermatoscopy attachment. The goal is to improve a diverse representation of data in terms of image quality, magnification, and resolution. The overview of data collection is shown in Fig. 1.

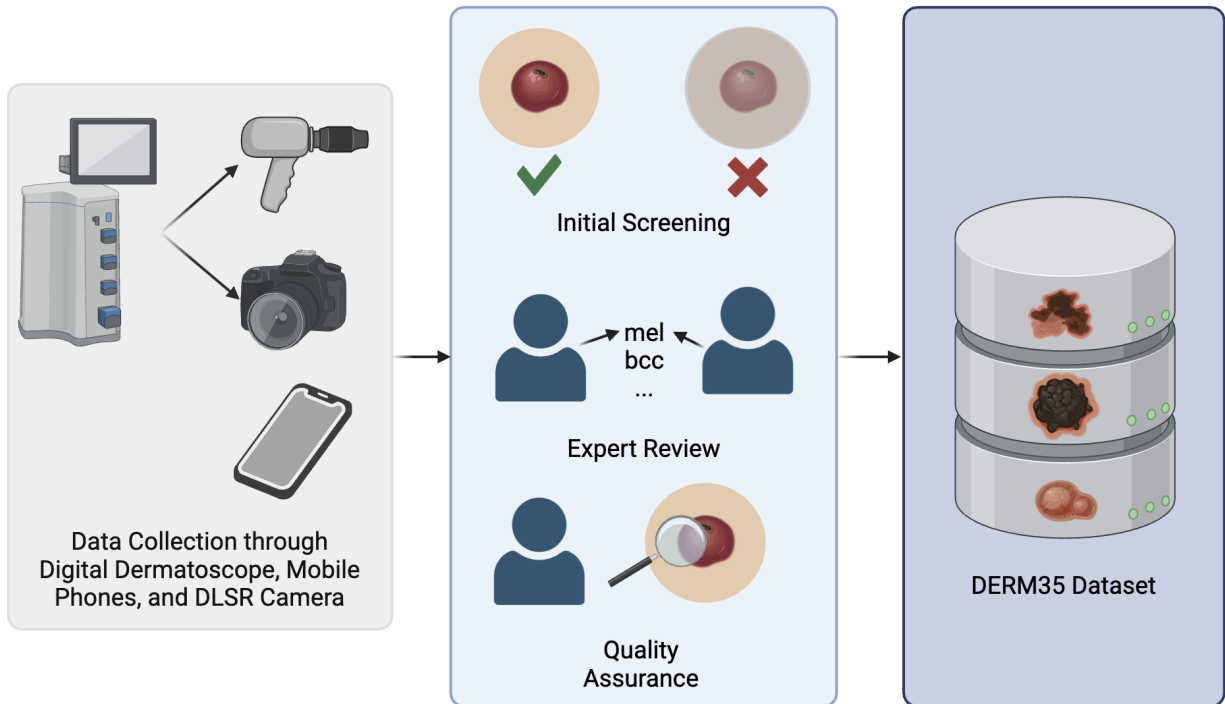


Figure 1: Shows an overview of the data collection procedure.

Data collection from digital dermatoscopy devices

Digital dermatoscopy devices are computer-attached systems and outfitted with dermatoscopes that utilize polarized light, enabling a magnification such as from 10x to 140x. This feature facilitates the thorough examination of deeper skin structures with a high level of detail. These dermatoscopy devices are linked to a computer system equipped with specialized software for the purpose of capturing and storing images. By using this software, dermatologists can follow up on the patients and their skin lesions with detailed information such as location and lesion classes. Each lesion is captured using a standardized technique and consistent lighting conditions to minimize any potential variability. Dermatoscopy is performed in the contact-polarized mode using an interface medium to avoid reflection caused by excessive scales, with ultrasound gel applied when necessary. The dermatologists ensure the most possible and accurate alignment of the field of view, with the lesion at the center and a small margin of surrounding healthy skin included to provide contextual information. To generate our dataset, we exported the data using their software tools in suitable formats such as HTML files. The raw data was subsequently retrieved from the raw files as lesion images and their metadata information. The cases were selected from this system by two expert dermatologists according to their consensus benign diagnosis, follow-up, and excised lesions with a histopathologic report.

Data collection from mobile phones and hand-held dermatoscopes

Mobile phone integrated dermatoscopes are low-cost and accessible devices that can provide state-of-art image quality. In this dataset, Apple iPhone 5 and 7, equipped with a 3gen Dermlite DL 4 hand-held dermatoscope kits, were used to collect dermatoscopic images. The Dermlite DL4 attachment with mobile devices enables the utilization of polarized light dermatoscopy, which offers a maximum magnification of 10x. The use of high-level magnification is essential for thoroughly analyzing the intricate components of the skin. The mobile phone was utilized alongside dermatoscope attachments, facilitating the acquisition of high-resolution (such as at 3840x2160 pixels, 4K resolution) skin lesion photos directly onto the phone. The mobile photos, along with their metadata, including lesion classes, were systematically documented, and matched with their records on digital dermatoscopy devices. A standardized image acquisition process was adhered to keep consistent lighting and framing conditions for all photos. The dermatologists conducted the imaging by positioning the lesions in the center of the field of view as possible while also including a border of healthy skin to offer contextual information. When focusing or centering the mobile phone camera was challenging, the dermatologists took photos in different angles. This usually caused the edges of the dermatoscopes as a

large black region to be visible on these images. These black regions were cropped from the images meticulously to increase standardization of images.

Data selection and quality control

The raw dataset included not only dermatoscopic images but also non-dermatoscopic images and other images such as device test images. To accelerate the data selection procedure, the dermatoscopic images were extracted by utilizing a script in Python (version: 3.11.5) that selected the images together with their metadata information. The BeautifulSoup library (version: 4.12.2) was utilized for the automated extraction and categorization of photos in HTML format. Data that could not be extracted or exported automatically in HTML format was hand-labeled and classified. The metadata was additionally stored manually in comma-separated values (CSV) files. To remove duplicate images, their file sizes were compared by using a script coded in Python. These scripts found 280 duplicate images. Then, they were manually reviewed. Consequently, all dermatoscopic images were retrieved and their corresponding information was stored in a CSV file. After automated extraction of the images, the careful selection of data was facilitated to maintain the integrity and usefulness of the dataset for both clinical reference and computational purposes. The criteria for selection were determined prior to the initiation of data collection and were consistently followed during the selection procedure.

Inclusion Criteria

- **Image Quality:** Images must be clear, in focus, and have sufficient quality. All images were reviewed manually to ensure that key diagnostic features of the skin lesions are understandable.
- **Diagnostic Confirmation:** Only images of lesions with a consensus of clinical diagnosis by two expert dermatologists or a histopathological confirmation (where available) were included.

Exclusion Criteria

- **Poor Image Quality:** Images that were blurred, under- or over-exposed, or had large artifacts. All images were reviewed manually, and the images that could potentially interfere with diagnosis were excluded.
- **Incomplete Data:** Images lacking essential metadata such as the presumed diagnosis were not included in the dataset.
- **Ethical Concerns:** Images that contained identifiable patient information or did not have proper consent were excluded to uphold ethical standards.
- **Unsuitable:** Images which contain unsuitable skin diseases or artefacts were excluded. Nail lesions, mucosal lesions, cockade nevus, leukoplakia, sarcoidosis psoriasis, verruca, cyst, keloid, sebaceous hyperplasia, wart, genital wart, lipoid proteinoz, subcorneal hemorrhage, pigmented purpuric dermatosis, mucosal melanosis, pygmented bowen, verruca, sarkoidoz psoriasis, and some types of adenocarcinoma such as sebaceous carcinoma and eccrine glands were excluded.

Selection Process The selection process involved multiple stages:

- **Initial Screening:** A preliminary review of images was conducted by trained engineers to remove images that obviously did not meet the inclusion and exclusion criteria. If one more than different classes of skin lesion is located in an image, these images are cropped.
- **Expert Review:** Two expert dermatologists then reviewed the remaining images to ensure that they met the clinical standards and diagnostic requirements.
- **Quality Assurance:** A final review was conducted by a panel comprising two dermatologists (GG and SPY with over 20 years experience on dermatoscopy) to ensure the images were of suitable quality for both clinical reference and computational tasks.

Data Records

All images are in JPEG format with their corresponding label in metadata. The metadata file was generated in CSV file to process easily. The metadata contains file names and lesion classes with their detailed taxonomic identification.

A three-level taxonomy tree following the latest dermatological classification standards [28] was created to guide the use of DERM38. The benign skin lesions that are high risk of being or becoming malignant were especially classified into a separate subclass such as dysplastic nevus [29], congenital nevus [30], blue nevus [31] and recurrent nevus that have the risk of unremoved malignant cell. The skin lesions were classified according to their specific anatomical localizations

Table 1: The DERM38 dataset contains 12,345 skin lesions divided into 5 super classes, 15 main classes, and 38 subclasses.

Superclass	Mainclass	Subclass	# of Images
Melanocytic Benign	Banal Compound	Acral (an)	22
		Congenital (con)	423
		Miescher (mn)	38
		Nevus (cn)	673
	Banal Dermal	Blue (bn)	156
		Nevus (dn)	539
	Banal Junctional	Acral (an)	351
Congenital (con)		145	
Nevus (jn)		1419	
Lentigo	Ink Spot Lentigo (isl)	6	
	Lentigo Simplex (ls)	23	
	Solar Lentigo (sl)	65	
Dysplastic Compound	Acral (an)	8	
	Congenital (con)	30	
	Nevus (cn)	426	
Dysplastic Junctional	Acral (an)	212	
	Spitz (sn)	10	
	Nevus (jn)	5465	
Dysplastic Recurrent	Recurrent (rn)	15	
Melanocytic Malignant	Melanoma	Acral Nodular (anm)	78
		Acral Lentiginous (alm)	54
		Lentigo Maligna (lm)	85
		Lentigo Maligna Melanom (lmm)	21
		Melanoma (mel)	164
Nonmelanocytic Benign	Keratinocytic	Seborrheic Keratosis (sk)	632
		Lichenoid Keratosis (lk)	6
	Skin Appendages	Dermatofibroma (df)	173
	Vascular	Hemangioma (ha)	269
Lymphangioma (la)		10	
Pyogenic Granuloma (pg)		7	
Nonmelanocytic Indeterminate	Keratinocytic	Actinic Keratosis (ak)	48
Nonmelanocytic Malignant	Keratinocytic	Basal Cell Carcinoma (bcc)	423
		Bowen's Disease (bd)	46
		Cutaneous Horn (ch)	9
		Mammary Paget Disease (mpd)	13
		Squamous Cell Carcinoma (scc)	263
	Skin Appendages	Dermatofibrosarcoma Protuberans (dfsp)	4
Vascular	Kaposi Sarcoma (ks)	14	
Total			12,345

such as palm-sole (acral), face and trunk-extremities. Combined lesions with multiple pathological classification were excluded if cropping into separate images is not possible. Skin lesions were initially grouped into the two classes as melanocytic and non-melanocytic. These two classes were further divided into malignant, indeterminate and benign groups, and five super classes were created. These five super classes were then divided into 15 main classes. Lastly, sub-lesion types were then classified into 38 different subclasses. Melanocytic-benign lesions were classified into lentigo with ink spot lentigo (isl), lentigo simplex (ls), and solar lentigo (sl) subclasses, banal with dermal, compound, and junctional subclasses and dysplastic with compound, junctional, and recurrent (rn) subclasses. Dysplastic dermal nevus were added into banal dermal nevus because of their similar patterns. Common nevus subclasses (acral (an), blue (bn), Miescher (mn), congenital (cn), and spitz/reed (sn) nevus) under dermal, compound, and junctional groups were then classified into their subclasses if available. Melanoma (mel) was classified under melanocytic-malignant lesions, with five further subclasses as acral nodular melanoma (anm), acral lentiginous melanoma (alm), lentigo maligna (lm), lentigo maligna melanoma (lmm), and melanoma (mel). Nonmelanocytic-benign lesions were classified into two subclasses as keratinocytes (lichenoid keratosis (lk), seborrheic keratosis (sk)), skin appendages (dermatofibroma (df)), and vascular (hemangioma (ha), lymphangioma (la), and pyogenic granuloma (pg)). Nonmelanocytic-malignant lesions were classified into three subclasses as keratinocytes (basal cell carcinoma (bcc), Bowen’s disease (bd), cutaneous horn (ch), mammary Paget disease (mpd), and squamous cell carcinoma (scc)), skin appendages (dermatofibrosarcoma protuberans (dfsp)), and vascular (Kaposi sarcoma (ks)). In addition, actinic keratosis (ak) was classified under nonmelanocytic-indeterminate subclasses. The taxonomy tree of these classes and their sizes were shown in Fig. 2 and Table 1, respectively.

Technical Validation

All images in this dataset were of patients applying to the dermatology department with skin complaints. All lesions were classified and reviewed according to the rules of dermatoscopic evaluation by two expert dermatologists in a consensus decision. All malignant skin lesions were all biopsy proven. The majority of these lesions consisted of follow-up images and were labeled using patient records. Nevus with over 2 years of digital dermatoscopic follow-up were annotated with no change except nevoid involution. The number of dysplastic nevus (N: 6,157) constituted a large part of the dataset. These dysplastic nevi were followed up in daily clinical practice rather than banal nevus (N:3,764). Malignant forms of benign lesions such as dfsp (N:4, counterpart of df) were also included in the dataset, even if the number of data is small. Early forms of malignant tumors such as mpd and bd which are a type of intraepidermal scc were also included. The consensus of GG and SPY experts labeled all the benign images that did not have histology or further follow-up. GG (with second Ph.D. in Basic Oncology) and SPY are two expert dermatologists with 20+ years of experience in dermatology.

Usage Notes

The dataset provided in this study represents the initial comprehensive collection of skin lesion data from Türkiye, serving as a distinctive and important asset for both the medical and machine learning fields. The launch of this dataset represents a notable progression, especially when considering the wide range of skin types, it addresses and the comprehensive classification of skin lesions it contains. The dataset is valuable due to the inclusion of various benign subclasses that closely resemble malignant tumors, distinguishing it from current collections and presenting a novel opportunity for the advancement of advanced diagnostic algorithms.

The absence of a rich sub-classification may result in misclassification. For instance, congenital nevus (which is not categorized as a separate subclass in the published datasets) can often be mistaken as a melanoma [30]. It is also important to know that the lesion is a congenital nevus as this lesion has a high risk of evolving into a melanoma [30]. We also included uncommon lesions that are difficult to collect or annotate such as spitz/reed nevus [32]. By using our detailed subclassification, this dataset enables researchers to develop and refine more reliable AI models capable of distinguishing benign from malignant ones, improving diagnostic accuracy and reducing the likelihood of misdiagnosis. The dataset includes 38 subclasses, allowing researchers to focus on more intelligent algorithms such as hierarchical learning [33].

The dataset exhibits potential to serve as a fundamental component in the advancement of effective algorithms for identifying malignant skin lesions. The ongoing obstacle in dermatological diagnosis lies in the difficulty of differentiating between benign and malignant forms, particularly when they exhibit comparable visual characteristics. The incorporation of benign that exhibit similarities to malignant counterparts in this collection of data presents a potential for enhancing the precision of machine learning algorithms. Therefore, it is anticipated that this technology will facilitate progress in the early and accurate detection of diseases, potentially mitigating the occurrence of false positive results and ultimately enhancing patient prognoses.

The inclusion of the dataset originating from Türkiye contributes to the expansion of the worldwide data repository, which has historically been underrepresented in this research domain. The geographical specificity of this information is of great use to academics who seek to create diagnostic models that are both resilient and efficient across various ethnicities and geographic areas. Additionally, it functions as a valuable resource for doctors who aim to comprehend the diversity in lesion, which can be impacted by various factors such as regional environmental conditions and genetic predispositions.

Clinicians are encouraged to employ this dataset as a visual resource for the identification of skin lesions, while researchers are encouraged to utilize it for comparative analyses with other datasets specific to the location. This dataset is of particular utility to machine learning practitioners for the purposes of training and verifying classification algorithms. The comprehensive depiction of complex instances within the dataset offers a rigorous platform for evaluating algorithms intended to distinguish between benign and malignant tumors.

In brief, this dataset serves to enhance the existing body of data pertaining to skin lesions, while also paving the way for the development of sophisticated diagnostic instruments. We anticipate that this tool will be a helpful resource in enhancing the precision and effectiveness of skin cancer detection and diagnosis among various demographic groups.

In this dataset, there are 38 subgroup lesions. Brief descriptions of these subgroups presented below can be useful for AI researchers:

I. Melanocytic lesions: Originates from melanocytes, often pigmented, shades of brown, black, tan, blue. Reflecting varying concentrations and depth of melanin within the skin.

1. Benign: Non-cancerous melanocyte-origin moles, generally harmless.

- (a) Dysplastic Nevus: Also known as atypical or Clark's nevus. They are characterized by histologic features, and they may appear small and banal clinically. Dysplastic nevi demonstrate the following clinical features: usually > 5 mm, irregular borders, some with a pigmented and erythematous rim, and variegated pigmentation with a mixture of pink, light and dark brown colors [34, 35]. This subclass contains compound nevus with acral and congenital subclasses, junctional nevus with acral and spitz/reed subclasses, and recurrent nevus.
- (b) Banal Nevus: A banal nevus, commonly known as a common mole, is a typical, non-cancerous skin mole that usually appears as a small, regular, round, or oval spot. Brown, tan, or pink, and may be either flat or slightly raised. This subclass contains dermal nevus with blue subclass, compound nevus with acral, Miescher, and congenital subclasses, and junctional nevus with acral and spitz/reed subclasses.
- (c) Lentigo: Pigmented and uniform. It is related to increasing of melanin expression by melanocytes. This subclass contains ink spot lentigo, lentigo simplex, and solar lentigo.
 - i. Compound (cn): Common mole, partially flat and partially elevated. Mix of dermal and epidermal melanocytes.
 - ii. Dermal (dn): Common mole. Raised bump, flesh-colored or brown mole. Located within the dermis. Generally benign. Unna nevus is included.
 - iii. Junctional (jn): Flat, typically dark, or brown mole. Occurs at epidermis-dermis junction.
 - iv. Recurrent nevus (rn): Incompletely removed nevus. Mole regrowth at previously excised site. Typically, benign. Can be confused with melanoma.
 - A. Acral nevus (an): Mole on palms or soles. Usually benign and characterized by their distinctive location on the body where the skin is thicker.
 - B. Blue nevus (bn): Deeply pigmented mole, blue-black color. Originates from deep dermal melanocytes. Usually, benign.
 - C. Congenital nevus (con): Mole present at birth and can grow proportionally with the child. Varies in size; potentially large. Increased melanoma risk later in life. Nevus spilus is included.
 - D. Ink Spot Lentigo (isl): Small, dark brown to black spots, resembling ink spots.
 - E. Lentigo Simplex (ls): Small, a precursor to junctional nevus. Small, flat, and typically darker spot. Also known as simple lentigo.
 - F. Miescher nevus (mn): Reveal pseudo network around hair follicles. Commonly benign, typically brown.
 - G. Solar Lentigo (sl): Larger, a precursor to seborrheic keratosis. Sun exposed.
 - H. Spitz/Reed nevus (sn): Raised, pink, red or brown mole. Often mistaken for melanoma. Typically, benign in children. Sometimes, shows a starburst pattern.

2. Malign: Cancerous growth from melanocytes. High risk of spreading.

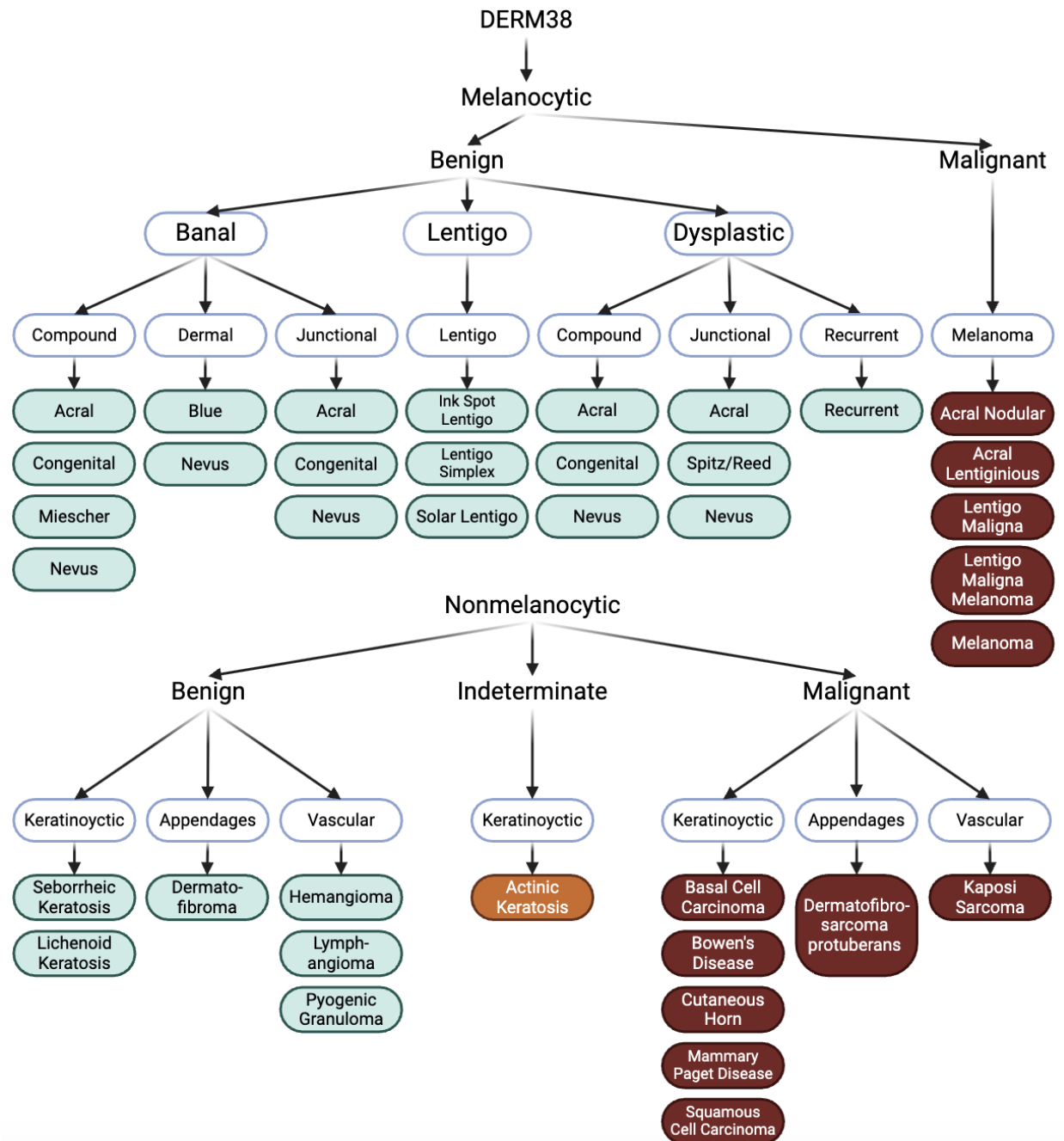


Figure 2: Shows an overview of the taxonomy tree. The first level includes the melanocytic and nonmelanocytic. The second level comprises malignant and benign groups of the first level. The third level is banal, dysplastic and lentigo for melanocytic benign, melanoma for melanocytic malignant, keratinocytic, skin appendages, vascular for nonmelanocytic benign, keratinocytic for nonmelanocytic-indeterminate, and keratinocytic, skin appendages, and vascular for nonmelanocytic malignant. The fourth level is the subclasses of related to their main and super classes. Our taxonomy tree contains 5 super classes, 15 main classes, and 38 subclasses.

- (a) Melanoma: Aggressive skin cancer. Arises from melanocytes. High risk of metastasis.
- i. Acral nodular melanoma (anm): Nodular melanoma form on poles and soles.
 - ii. Acral lentiginous melanoma (alm): A rare subtype of melanoma. Lentiginous form on poles and soles.

- iii. Lentigo maligna (lm): Larger, a precursor to lentigo maligna melanoma. Slow-growing skin cancer. Appears as a flat, blotchy patch. Early form of melanoma. Located on sun-exposed areas of the skin.
- iv. Lentigo maligna melanoma (lmm): Various number of colors, especially blue or black that means the melanoma cells have reached to the deeper layers of skin.
- v. Melanoma (mel): Melanoma can appear as a new dark spot on the skin or from an existing mole that changes in color, size, or feel. It can spread quickly to other parts of the body and is critical to treat early.

II. Nonmelanocytic lesions: Uncontrollable growth pattern from keratinocytes, fibroblasts, or vascular cells.

1. Benign: Non-cancerous growths from keratinocytes, fibroblasts, or vascular cells.

(a) Keratinocytic:

- i. Seborrheic keratosis (sk): Appears as a waxy, wart-like, often brown or black growth. Commonly has a rough texture. Stucco keratosis is included which is located on legs.
- ii. Lichenoid keratosis (lk): Inflammatory and regressing on solar lentigo and seborrheic keratosis.

(b) Skin appendages:

- i. Dermatofibroma (df): Firm, benign skin nodule. Common on legs or arms. Typically, brownish, and harmless.

(c) Vascular:

- i. Hemangioma (ha): Bright red, raised birthmark. Made of clustered blood vessels. Common in infants, usually fades.
- ii. Lymphangioma (la): Rare, soft, often translucent mass. Appears as a swelling on the skin or mucous membranes. Typically seen in infants.
- iii. Pyogenic granuloma (pg): Small, reddish, raised lesion. Prone to bleeding and rapid growth. Often appears after skin injury.

2. Indeterminate: Not exactly categorized as benign or malignant. This does not imply that these lesions are malignant.

(a) Keratinocytic:

- i. Actinic keratosis (ak): Rough, scaly skin patch. Sun-induced, precancerous. Common on sun-exposed areas. 20% malignancy risk.

3. Malign: Cancerous growths, and can originate from keratinocytes, vascular, or connective tissue cells.

(a) Keratinocytic:

- i. Basal cell carcinoma (bcc): Appears as a shiny, pearly bump or a flat, scar-like lesion. Most common on sun-exposed areas. Slow growing rarely metastasizes.
- ii. Bowen's disease (bd): Early form of scc. Appears as a persistent, red, scaly patch. Can resemble eczema or psoriasis. Often occurs on sun-exposed skin.
- iii. Cutaneous horn (ch): Hard, protruding growth resembling an animal horn. Composed of compacted keratin mostly located on the face, ears, and other sun exposed areas. It may be associated with benign, premalignant, and malignant lesions. Often benign, base may have underlying malignancy. Only early form of scc is included.
- iv. Mammary Paget's Disease (mpd): Early form of scc and a type of breast cancer. mpd need to be diagnosis before it converts to nodular form.
- v. Squamous cell carcinoma (scc): Common, appears as a firm, red nodule, or a flat lesion with a scaly, crusted surface. Commonly develops in sun-exposed areas. Can be ulcerative and may bleed.

(b) Skin appendages:

- i. Dermatofibrosarcoma protuberans (dfsp): Rare, appears as a deep-seated, firm lump under the skin. Often starts as a small, painless nodule that gradually enlarges. Typically develops on the trunk or limbs.

(c) Vascular:

- i. Kaposi sarcoma (ks): Presents as purple, red, or brown blotches or tumors on the skin. It is originated from vessel's endothelial cells.

References

- [1] Philipp Tschandl, Christoph Rinner, Zoe Apalla, Giuseppe Argenziano, Noel Codella, Allan Halpern, Monika Janda, Aimilios Lallas, Caterina Longo, Josep Malvehy, et al. Human–computer collaboration for skin cancer recognition. *Nature Medicine*, 26(8):1229–1234, 2020.
- [2] David Gutman, Noel CF Codella, Emre Celebi, Brian Helba, Michael Marchetti, Nabin Mishra, and Allan Halpern. Skin lesion analysis toward melanoma detection: A challenge at the international symposium on biomedical imaging (isbi) 2016, hosted by the international skin imaging collaboration (isic). *arXiv preprint arXiv:1605.01397*, 2016.
- [3] Noel CF Codella, David Gutman, M Emre Celebi, Brian Helba, Michael A Marchetti, Stephen W Dusza, Aadi Kallou, Konstantinos Liopyris, Nabin Mishra, Harald Kittler, et al. Skin lesion analysis toward melanoma detection: A challenge at the 2017 international symposium on biomedical imaging (isbi), hosted by the international skin imaging collaboration (isic). In *2018 IEEE 15th international symposium on biomedical imaging (ISBI 2018)*, pages 168–172. IEEE, 2018.
- [4] Philipp Tschandl, Cliff Rosendahl, and Harald Kittler. The ham10000 dataset, a large collection of multi-source dermatoscopic images of common pigmented skin lesions. *Scientific data*, 5(1):1–9, 2018.
- [5] Marc Combalia, Noel CF Codella, Veronica Rotemberg, Brian Helba, Veronica Vilaplana, Ofer Reiter, Cristina Carrera, Alicia Barreiro, Allan C Halpern, Susana Puig, et al. Bcn20000: Dermoscopic lesions in the wild. *arXiv preprint arXiv:1908.02288*, 2019.
- [6] María Agustina Ricci Lara, María Victoria Rodríguez Kowalczyk, Maite Lisa Eliceche, María Guillermina Ferraresso, Daniel Roberto Luna, Sonia Elizabeth Benitez, and Luis Daniel Mazzuocolo. A dataset of skin lesion images collected in argentina for the evaluation of ai tools in this population. *Scientific Data*, 10(1):712, 2023.
- [7] Michael A Marchetti, Emily A Cowen, Nicholas R Kurtansky, Jochen Weber, Megan Dauscher, Jennifer DeFazio, Liang Deng, Stephen W Dusza, Helen Haliasos, Allan C Halpern, et al. Prospective validation of dermoscopy-based open-source artificial intelligence for melanoma diagnosis (prove-ai study). *NPJ Digital Medicine*, 6(1):127, 2023.
- [8] Giuseppe Argenziano, H Peter Soyer, Vincenzo De Giorgio, Domenico Piccolo, Paolo Carli, Mario Delfino, Angela Ferrari, Rainer Hofmann-Wellenhof, Daniela Massi, Giampero Mazzocchetti, et al. Interactive atlas of dermoscopy. 2000.
- [9] Dermofit library: A cognitive prosthesis to aid focal skin lesion diagnosis. <https://homepages.inf.ed.ac.uk/rbf/DERMOFIT/>.
- [10] Ioannis Giotis, Nynke Molders, Sander Land, Michael Biehl, Marcel F Jonkman, and Nicolai Petkov. Med-node: A computer-assisted melanoma diagnosis system using non-dermoscopic images. *Expert systems with applications*, 42(19):6578–6585, 2015.
- [11] Seung Seog Han, Myoung Shin Kim, Woohyung Lim, Gyeong Hun Park, Ilwoo Park, and Sung Eun Chang. Classification of the clinical images for benign and malignant cutaneous tumors using a deep learning algorithm. *Journal of Investigative Dermatology*, 138(7):1529–1538, 2018.
- [12] Xiaoxiao Sun, Jufeng Yang, Ming Sun, and Kai Wang. A benchmark for automatic visual classification of clinical skin disease images. In *European Conference on Computer Vision*, pages 206–222. Springer, 2016.
- [13] Jufeng Yang, Xiaoxiao Sun, Jie Liang, and Paul L Rosin. Clinical skin lesion diagnosis using representations inspired by dermatologist criteria. In *Proceedings of the IEEE Conference on Computer Vision and Pattern Recognition*, pages 1258–1266, 2018.
- [14] Jufeng Yang, Xiaoping Wu, Jie Liang, Xiaoxiao Sun, Ming-Ming Cheng, Paul L Rosin, and Liang Wang. Self-paced balance learning for clinical skin disease recognition. *IEEE transactions on neural networks and learning systems*, 31(8):2832–2846, 2019.
- [15] Andre GC Pacheco, Gustavo R Lima, Amanda S Salomao, Breno Krohling, Igor P Biral, Gabriel G de Angelo, Fábio CR Alves Jr, José GM Esgario, Alana C Simora, Pedro BC Castro, et al. Pad-ufes-20: A skin lesion dataset composed of patient data and clinical images collected from smartphones. *Data in brief*, 32:106221, 2020.
- [16] Abbi Ward, Jimmy Li, Julie Wang, Sriram Lakshminarasimhan, Ashley Carrick, Bilson Campana, Jay Hartford, Pradeep Kumar S, Tiya Tiyasirichokchai, Sunny Virmani, Renee Wong, Yossi Matias, Greg S. Corrado, Dale R. Webster, Dawn Siegel, Steven Lin, Justin Ko, Alan Karthikesalingam, Christopher Semturs, and Pooja Rao. Crowdsourcing dermatology images with google search ads: Creating a real-world skin condition dataset, 2024.
- [17] Samuel Freire da Silva. Atlas dermatologico. <http://atlasdermatologico.com.br/>.

- [18] Jehad Amin AlKattash. Dermaamin. <https://www.dermaamin.com/site/>.
- [19] Matthew Groh, Caleb Harris, Luis Soenksen, Felix Lau, Rachel Han, Aerin Kim, Arash Koochek, and Omar Badri. Evaluating deep neural networks trained on clinical images in dermatology with the fitzpatrick 17k dataset. In *Proceedings of the IEEE/CVF Conference on Computer Vision and Pattern Recognition*, pages 1820–1828, 2021.
- [20] Roxana Daneshjou, Kailas Vodrahalli, Roberto A. Novoa, Melissa Jenkins, Weixin Liang, Veronica Rotemberg, Justin Ko, Susan M. Swetter, Elizabeth E. Bailey, Olivier Gevaert, Pritam Mukherjee, Michelle Phung, Kiana Yekrang, Bradley Fong, Rachna Sahasrabudhe, Johan A. C. Allerup, Utako Okata-Karigane, James Zou, and Albert S. Chiou. Disparities in dermatology ai performance on a diverse, curated clinical image set. *Science Advances*, 8(32):eabq6147, 2022.
- [21] The cancer genome atlas. <https://www.cancer.gov/about-nci/organization/ccg/research/structural-genomics/tcga>.
- [22] Dermnet nz dataset. <https://www.dermnetnz.org/>.
- [23] Jordan Yap, William Yolland, and Philipp Tschandl. Multimodal skin lesion classification using deep learning. *Experimental dermatology*, 27(11):1261–1267, 2018.
- [24] Teresa Mendonça, Pedro M Ferreira, Jorge S Marques, André RS Marcal, and Jorge Rozeira. Ph 2-a dermoscopic image database for research and benchmarking. In *2013 35th annual international conference of the IEEE engineering in medicine and biology society (EMBC)*, pages 5437–5440. IEEE, 2013.
- [25] Jeremy Kawahara, Sara Daneshvar, Giuseppe Argenziano, and Ghassan Hamarneh. Seven-point checklist and skin lesion classification using multitask multimodal neural nets. *IEEE journal of biomedical and health informatics*, 23(2):538–546, 2018.
- [26] Noel Codella, Veronica Rotemberg, Philipp Tschandl, M Emre Celebi, Stephen Dusza, David Gutman, Brian Helba, Aadi Kalloo, Konstantinos Liopyris, Michael Marchetti, et al. Skin lesion analysis toward melanoma detection 2018: A challenge hosted by the international skin imaging collaboration (isic). *arXiv preprint arXiv:1902.03368*, 2019.
- [27] Veronica Rotemberg, Nicholas Kurtansky, Brigid Betz-Stablein, Liam Caffery, Emmanouil Chousakos, Noel Codella, Marc Combalia, Stephen Dusza, Pascale Guitera, David Gutman, et al. A patient-centric dataset of images and metadata for identifying melanomas using clinical context. *Scientific data*, 8(1):1–8, 2021.
- [28] Alon Scope, Konstantinos Liopyris, Jochen Weber, Raymond L Barnhill, Ralph P Braun, Clara N Curiel-Lewandrowski, David E Elder, Gerardo Ferrara, Jane M Grant-Kels, Thiago Jeunon, et al. International skin imaging collaboration-designated diagnoses (isic-dx): Consensus terminology for lesion diagnostic labeling. *Journal of the European Academy of Dermatology and Venereology*, 2024.
- [29] Dana Baigrie and Laura S Tanner. Dysplastic nevi. 2018.
- [30] VA Kinsler, P O’hare, N Bulstrode, JE Calonje, WK Chong, D Hargrave, T Jacques, D Lomas, NJ Sebire, and O Slater. Melanoma in congenital melanocytic naevi. *British Journal of Dermatology*, 176(5):1131–1143, 2017.
- [31] Luise Ribeiro Daltro, Lygia Bertalha Yaegashi, Rodrigo Abdalah Freitas, Bruno de Carvalho Fantini, and Cacilda da Silva Souza. Atypical cellular blue nevus or malignant blue nevus? *Anais Brasileiros de Dermatologia*, 92:110–112, 2017.
- [32] Tiffany W Cheng, Madeline C Ahern, and Alessio Giubellino. The spectrum of spitz melanocytic lesions: From morphologic diagnosis to molecular classification. *Frontiers in Oncology*, 12:889223, 2022.
- [33] Catarina Barata and Jorge S Marques. Deep learning for skin cancer diagnosis with hierarchical architectures. In *2019 IEEE 16th International Symposium on Biomedical Imaging (ISBI 2019)*, pages 841–845. IEEE, 2019.
- [34] Cristina Carrera and Ashfaq A Marghoob. Discriminating nevi from melanomas: clues and pitfalls. *Dermatologic clinics*, 34(4):395–409, 2016.
- [35] Kee Suck Suh, Jong Bin Park, Joon Hee Kim, Seol Hwa Seong, Ji Yun Jang, Myeong Hyeon Yang, and Min Soo Jang. Dysplastic nevus: Clinical features and usefulness of dermoscopy. *The Journal of Dermatology*, 46(2):e76–e77, 2018.

Acknowledgements

Abdurrahim Yilmaz has been funded by the President’s PhD Scholarships of Imperial College London.

All figures are created with BioRender.com.

Author contributions statement

Conceptualization, A.Y., S.P.Y., and G.G.; methodology, A.Y., G.G., and B.T.; software, A.Y.; validation, G.G., S.P.Y., and B.T.; formal analysis, A.Y.; investigation, G.G. and S.P.Y.; resources, G.G. and S.P.Y.; data curation, A.Y., G.G., S.P.Y., and B.T.; writing—original draft preparation, A.Y., and B.T.; writing—review and editing, A.Y. and G.G.; visualization, A.Y. All authors have read and agreed to the published version of the manuscript.

Competing interests

There is no competing interest.